Research Article

An IEEE 802.11 EDCA Model with Support for Analysing Networks with Misbehaving Nodes

Szymon Szott, Marek Natkaniec, and Andrzej R. Pach

Department of Telecommunications, AGH University of Science and Technology, Al. Mickiewicza 30, 30-059 Krakow, Poland

Correspondence should be addressed to Szymon Szott, szott@kt.agh.edu.pl

We present a novel model of IEEE 802.11 EDCA with support for analysing networks with misbehaving nodes. In particular, we consider backoff misbehaviour. Firstly, we verify the model by extensive simulation analysis and by comparing it to three other IEEE 802.11 models. The results show that our model behaves satisfactorily and outperforms other widely acknowledged models. Secondly, a comparison with simulation results in several scenarios with misbehaving nodes proves that our model performs correctly for these scenarios. The proposed model can, therefore, be considered as an original contribution to the area of EDCA models and backoff misbehaviour.

1. Introduction

The IEEE 802.11 standard [1] for wireless local area networks (WLANs) does not provide users with incentives to cooperate when accessing the shared radio channel. Therefore, misbehaviour, in the form of selfish parameter configuration, may become a serious problem. This is in particular true for Enhanced Distributed Channel Access (EDCA), one of the medium access functions of IEEE 802.11. EDCA provides Quality of Service (QoS) for WLANs through traffic differentiation. It defines new medium access parameters and, therefore, new opportunities to misbehave.

Misbehaviour in EDCA can occur by deliberately changing the medium access parameters defined in the standard in order to increase the chance of accessing the medium and, as a result, increase the misbehaving node's effective throughput. Though several parameters may be modified, we focus on changes to the backoff parameters (known as backoff misbehaviour) because this method is the most difficult to detect. Backoff misbehaviour is hidden from detection schemes working at the network layer and can be combined with misbehaviour in upper layers. It is easy to perform because the medium access function, which governs the backoff procedure, can be modified through the wireless card driver. The latest drivers, for example, [2], allow changing these parameters through the command line. Even

equipment vendors can make nonstandard modifications to increase the performance of their cards [3]. As numerous studies have shown, backoff misbehaviour is a serious threat for WLANs [4–6].

In this paper, we focus on the analytical modelling of EDCA networks with misbehaving nodes. Even though many EDCA models have already been presented in the literature (e.g., [7, 8]) none have studied misbehaviour. Furthermore, papers such as [9–12] use IEEE 802.11 models to study networks with misbehaving nodes; however, these are models of the Distributed Coordination Function (DCF), the predecessor of EDCA. Therefore, a new analytical model of EDCA is presented to study the impact of misbehaving nodes on network performance.

Our EDCA model is distinguished by the following set of features:

(i) support for the analysis of backoff misbehaviour,

(ii) support for saturation and nonsaturation network conditions,

(iii) standard-compliant EDCA parameters,

(iv) proper handling of frames (i.e., each transmission attempt results in either a *success*, a *collision* or a *blocked medium*),

(v) Arbitration InterFrame Space (AIFS) differentiation,

(vi) distinguishing between the busy medium and frame blocking probabilities.

We believe that this set of features as a whole is unique and provides an original contribution to the area of EDCA models and backoff misbehaviour. We verify the model by simulations and show that it outperforms three other IEEE 802.11 models. The presented model can be used in game theoretical analysis of IEEE 802.11 networks with misbehaving nodes (similarly to [10, 13]). It can also assist in the design of new EDCA-based medium access protocols resistant to the negative influence of misbehaving nodes.

The rest of the paper is organised as follows. Section 2 provides a brief description of EDCA and a list of the assumptions made. The analysis of the EDCA model and misbehaviour are provided in Sections 3 and 4, respectively. In Section 5, we compare simulation and analytical results to (a) verify that the model is correct, (b) show that it outperforms three other models, and (c) prove it can be used to analyse networks with misbehaving nodes. Finally, Section 6 concludes the paper. The nomenclature used throughout the paper is provided in at the end of the paper.

2. EDCA Description and Assumptions

In this section, we first briefly describe EDCA and then list the assumptions necessary to analyse EDCA.

EDCA introduces four Access Categories (ACs) to provide QoS through traffic differentiation. These categories are, from the highest priority: Voice (Vo), Video (Vi), Best effort (BE), and Background (BK). The medium contention rules for EDCA are similar to 802.11 DCF. Each frame arriving at the MAC layer is mapped, according to its priority, to an appropriate AC. There are four transmission queues; one for each AC (Figure 1). Traffic differentiation is achieved through medium access parameters which assume different values for each AC. These parameters are: the Arbitration InterFrame Space Number (AIFSN), as well as the Contention Window Minimum and Maximum values (CW$^{\text{MIN}}$ and CW$^{\text{MAX}}$). The standard also defines the Transmission Opportunity Limit (TXOP$_{\text{Limit}}$). However, it is an optional parameter and we do not consider it in this paper. We refer the reader to [14] for an example of including this parameter in the model.

The EDCA parameters influence the medium access in the following manner. For the ith AC, AIFS$_i$ is the parameter which determines how long the medium has to be idle before a transmission or backoff countdown can commence. It is calculated as

$$\text{AIFS}_i = \text{SIFS} + \text{AIFSN}_i \cdot T_e, \qquad (1)$$

where T_e is the length of the slot time and SIFS is the Short Interframe Space of DCF. After a collision has occurred, the medium has to be idle not for an AIFS$_i$ but for an EIFS−DIFS (Extended/DCF Interframe Space) period. EIFS is calculated as SIFS + DIFS + ACKTxTime. This is the time required to transmit an ACK frame at the lowest PHY mandatory rate.

According to the backoff procedure, for the ith AC and jth retransmission attempt, a node randomly selects
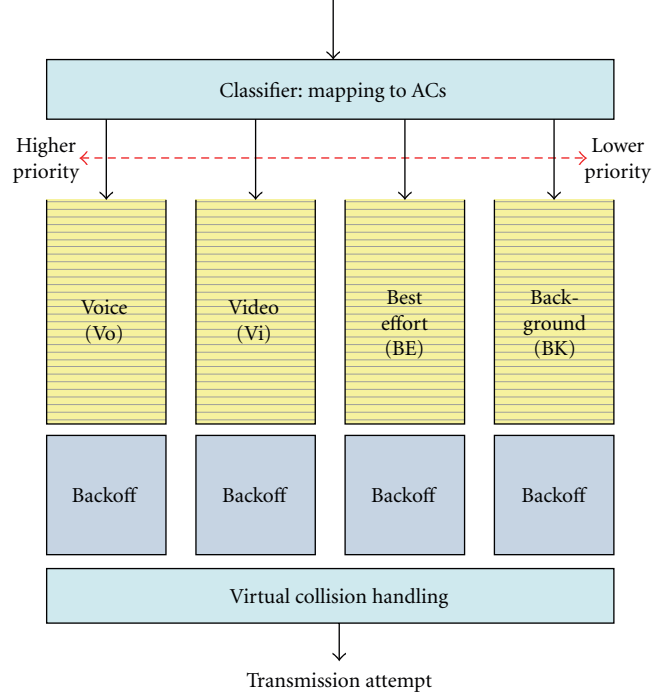

FIGURE 1: Mapping to ACs in EDCA [1].

TABLE 1: Default EDCA parameters of IEEE 802.11 HR/DSSS (802.11b).

Access category (i)	AIFSN$_i$	CW$_i^{\text{MIN}}$	CW$_i^{\text{MAX}}$
Vo	2	7	15
Vi	2	15	31
BE	3	31	1023
BK	7	31	1023

an integer value from the range $[0, \text{CW}_{i,j}]$. The contention window $\text{CW}_{i,j}$ is calculated as

$$\text{CW}_{i,j} = \min\left[2^j \cdot \left(\text{CW}_i^{\text{MIN}} + 1\right) - 1, \text{CW}_i^{\text{MAX}}\right],$$
$$i \in 0, \dots, N_{c-1}, \ j \in 0, \dots, M, \qquad (2)$$

where N_C is the number of ACs and M is the retransmission limit. After the Mth retransmission attempt the frame is dropped.

Table 1 contains the standard values of the EDCA parameters for IEEE 802.11 HR/DSSS (known as 802.11b) [1]. Furthermore, for 802.11b the standard defines $N_C = 4$, M equal to 4 or 7 (depending on frame length), SIFS = 10 μs, DIFS = 50 μs, and $T_e = 20\,\mu$s.

We attempt to model EDCA under the following assumptions:

(i) traffic is generated with a Poisson distribution,

(ii) frames are of equal length,

(iii) there are M/G/1 queues in each node,

(iv) the RTS/CTS exchange is not used,

(v) the TXOP$_{\text{Limit}}$ parameter is not used,

(vi) the medium is error-free,

(vii) all nodes are in a single-hop network, and there are no hidden stations,

(viii) each node transmits data of only one AC—this simplifies the analysis, and it is a practical assumption that the misbehaving user wants to send a single type of data (support for multiple ACs per node can be easily added, e.g., as in [15]),

(ix) nodes misbehave only by changing CW$_i^{\text{MIN}}$, CW$_i^{\text{MAX}}$—such parameter modification can be easily performed with the use of the latest wireless drivers [2]. We do not consider more elaborate attacks because they are either difficult to perform (e.g., modifying the EDCA mechanism implemented in the wireless card drivers) or are related to higher layers of the OSI model (e.g., swapping of ACs, node collusion) and thus out of the scope of the paper.

All these assumptions do not affect the analysis of misbehaviour because they influence the results in a quantitative (not qualitative) manner.

3. Model Analysis

The input parameters for our analysis of EDCA are:

(i) the number of ACs in the network (N_C),

(ii) the number of nodes using the ith AC (n_i),

(iii) the traffic rate of the ith AC given in frames per second (λ_i),

(iv) the average time required to send a DATA frame (T^{DATA}, based on the average frame size).

The goal of the analysis is to derive the overall throughput in each AC (S_i). It is defined as the quotient of the average duration of a successful transmission of a frame of the ith AC and the average duration of a contention slot (T^{CS}), in which the frame competes for medium access with other frames. Therefore, we have

$$S_i = \frac{p_i^S T^{\text{DATA}}}{T^{\text{CS}}}, \qquad (3)$$

where p_i^S is the is the probability of a successful transmission for the ith AC and T^{DATA} is the average time spent on transmitting a frame.

If we define τ_i as the transmission probability in a slot time for the ith AC, we can compute p_i^S as the probability that only one node is transmitting in a given slot time

$$p_i^S = n_i \, \tau_i \, (1 - \tau_i)^{n_i - 1} \prod_{j=0, j \neq i}^{N_c - 1} \left(1 - \tau_j\right)^{n_j}. \qquad (4)$$

We calculate T^{CS} using the following equation:

$$T^{\text{CS}} = \left(1 - p^B\right) T_e + P^S T^S + \left(p^B - P^S\right) T^C, \qquad (5)$$

where T_e is the slot time, T^S is the duration of a successful transmission, T^C is the duration of a collision, p^B is the probability of a busy channel, $1 - p^B$ is the probability of a free channel, and P^S is the overall probability of a successful transmission in any AC ($P^S = \sum_{i=0}^{N_c - 1} p_i^S$). We can now rewrite (3) as

$$S_i = \frac{p_i^S T^{\text{DATA}}}{(1 - p^B) T_e + P^S T^S + (p^B - P^S) T^C}. \qquad (6)$$

The time intervals T^S and T^C can be calculated as

$$T^S = \min[\text{AIFS}_i] + T^H + T^{\text{DATA}} + \text{SIFS} + T^{\text{ACK}} + 2\delta,$$

$$T^C = T^H + T^{\text{DATA}} + \delta + \text{ACK}_{\text{Timeout}} + \min[\text{AIFS}_i], \qquad (7)$$

where δ is the propagation delay, T^H is the time required to send the PHY and MAC headers, and ACK$_{\text{Timeout}}$ = EIFS $-$ DIFS.

The probability of a busy channel p^B is equal to the probability that at least one node is transmitting

$$p^B = 1 - \prod_{i=0}^{N_c - 1} (1 - \tau_i)^{n_i}. \qquad (8)$$

The remaining unknown variables of (4) and (6) can be found using analysis of the Markov chain presented in Figure 2. We assume that the events of frame generation, blocking, collision, and starting a frame transmission (defined below) are constant and independent from each other. This fundamental assumption, which follows from [16], allows us to use a Markov chain to model EDCA.

To describe the model, we introduce the following AC-dependent probabilities, each one calculated from the perspective of a given node (i.e., taking into account the perceived activity of other nodes).

(i) The frame blocking probability for the ith AC (p_i^B) is the probability that at least one other node is transmitting during the given node's backoff. Following the fundamental assumption of event independence it can be stated that each transmission "sees" the system in the steady state in which each of the other nodes transmits with a constant probability τ_i. Therefore, we need to take into account that $n_i - 1$ nodes in the ith AC may transmit and any of the nodes in the other ACs may transmit as well. Furthermore, we need to take into account the different values of AIFSN$_i$: nodes transmitting with a lower priority AC need to wait for more empty slots than nodes transmitting with a higher priority AC. We calculate p_i^B using the following equation:

$$p_i^B = 1 - \left[(1 - \tau_i)^{n_i - 1} \prod_{j=0, j \neq i}^{N_c - 1} \left(1 - \tau_j\right)^{n_j} \right]^{\text{AIFSN}_i - \text{AIFSN}^{\text{MIN}} + 1}, \qquad (9)$$

where $(1 - \tau_i)^{n_i - 1}$ is the probability that no other nodes using the ith AC are transmitting, $\prod_{j=0, j \neq i}^{N_c - 1} (1 - \tau_j)^{n_j}$ is the probability that no nodes using the other ACs are transmitting, and AIFSN$^{\text{MIN}}$ is the minimum AIFSN value among all ACs.
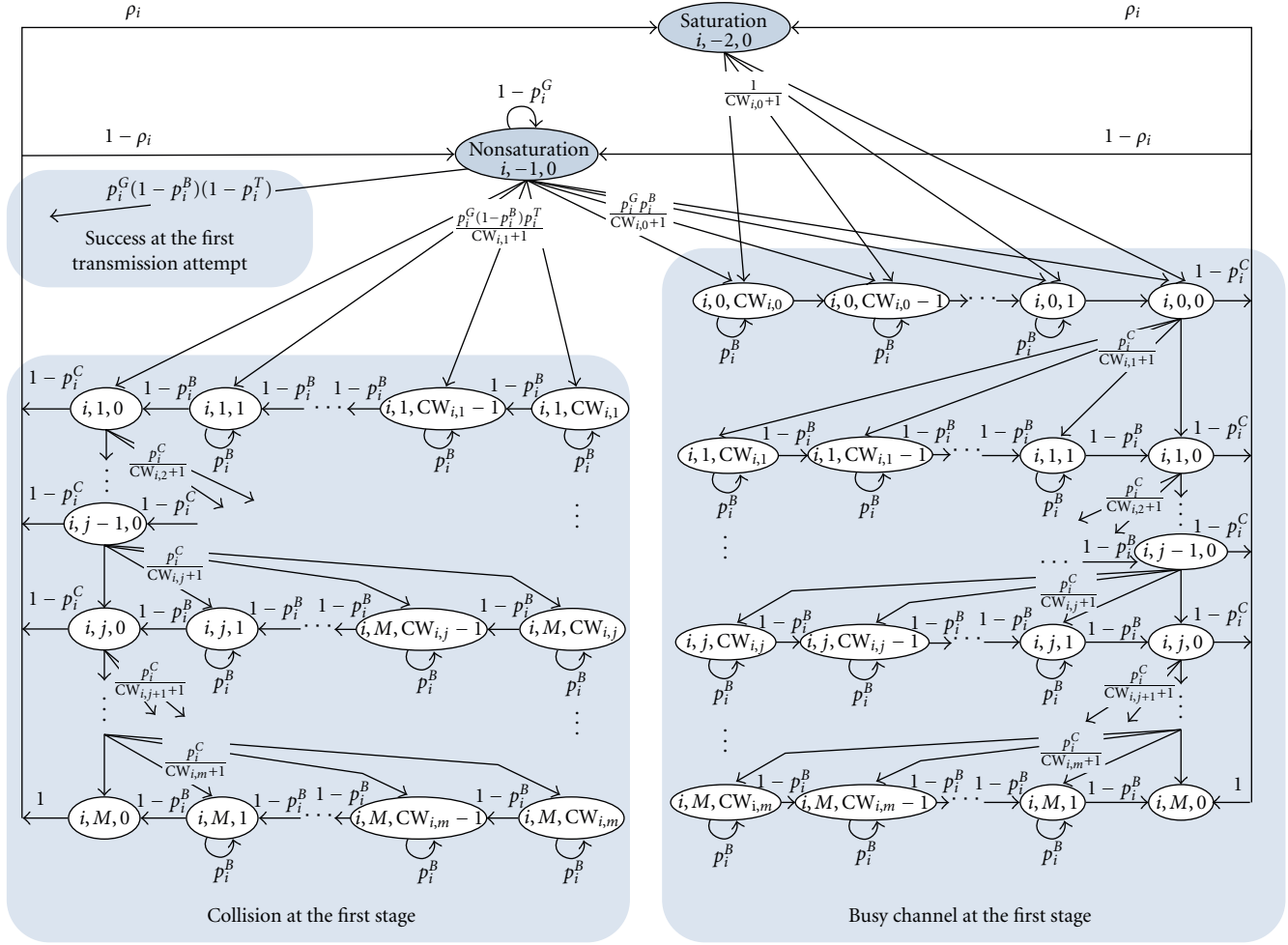
Figure 2: Markov chain of the proposed model.

(ii) The frame collision probability for the ith AC (p_i^C) is the probability that at least one other node is transmitting while the given node is transmitting

$$p_i^C = 1 - (1 - \tau_i)^{n_i - 1} \prod_{j=0, j \neq i}^{N_c - 1} \left(1 - \tau_j\right)^{n_j}. \qquad (10)$$

The difference between p_i^C and p_i^B is that in the former we do not need to take AIFS differentiation into account.

(iii) We denote the probability that at least one frame will arrive at the ith queue in a slot time as the frame generation probability (p_i^G)

$$p_i^G = 1 - e^{-\lambda_i T^{CS}}, \qquad (11)$$

where T^{CS} is the duration of a contention slot for the ith AC.

(iv) p_i^T is the probability that any other node will immediately begin its transmission (i.e., the probability of starting a frame transmission)

$$p_i^T = 1 - \left(1 - p_i^G\right)^{n_i - 1} \prod_{j=0, j \neq i}^{N_c - 1} \left(1 - p_j^G\right)^{n_j}. \qquad (12)$$

This situation occurs only under nonsaturation, when a frame is transmitted right after being generated.

(v) Finally, the saturation probability (ρ_i) is the probability that the ith queue is not empty after the previous transmission is finished

$$\rho_i = \lambda_i D_i, \qquad (13)$$

where D_i is the overall service time of a frame for the ith AC. A detailed description of this variable is given later.

Let us define $b_i(t)$ as the value of the backoff counter for a given node and the ith AC, where t is given in slot times. Furthermore, we define $s_i(t)$ as the backoff stage. Therefore,
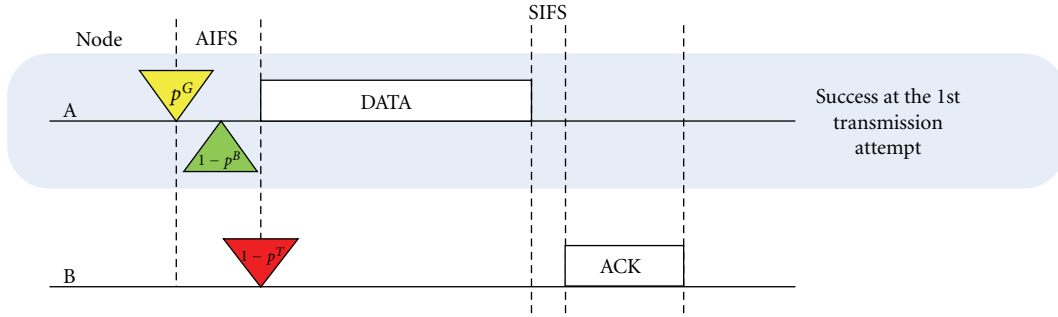
FIGURE 3: Diagram illustrating the action sequences related to a success at the 1st transmission attempt.

FIGURE 4: Diagram illustrating the action sequences related to a collision at the 1st stage.

we can model the bidimensional process $\{b_i(t), s_i(t)\}$ with the discrete Markov chain presented in Figure 2. We assume the notation that $b_{i,j,k} = \lim_{t \to \infty} P\{s_i(t) = j, b_i(t) = k\}$ ($i \in 0, \ldots, N_c - 1$, $j \in -2, \ldots, M$, and $k \in 0, \ldots, \mathrm{CW}_{i,j}$). These are the stationary distributions of the Markov chain. Furthermore, according to the Ergodic theorem "Any irreducible, finite, aperiodic Markov chain has a unique stationary distribution" [17] these stationary solutions are unique.

There are two special states in the model: for nonsaturation ($b_{i,-1,0}$) and saturation ($b_{i,-2,0}$) network conditions. A node remains in the former state waiting for a frame to be generated with the probability $1 - p_i^G$. However, it is impossible to remain in the latter state because the node immediately chooses a backoff value and enters one of the backoff states. The probability of entering the $b_{i,-1,0}$ and $b_{i,-2,0}$ states is related to ρ_i.

As can be seen from Figure 2, each transmission attempt results in either a *success at the first transmission attempt*, a *collision at the first stage* or a *busy channel at the first stage*. Diagrams illustrating the action sequences relevant to these three cases are presented in Figures 3, 4, and 5, respectively. To enable better understanding of the model the figures contain symbolic representations of probabilities. A successful transmission which does not require any backoff occurs in the nonsaturation case with a probability of $p_i^G(1 - p_i^B)(1 - p_i^T)$. If we consider only the case of a busy channel at the first stage, we have from the chain analysis

$$b_{i,0,0} = p_i^G p_i^B b_{i,-1,0} + b_{i,-2,0}, \tag{14}$$

where $b_{i,-1,0}$ represents the nonsaturation state and $b_{i,-2,0}$ represents the saturation state. Furthermore, every $b_{i,j,0}$ state can be represented as a function of $b_{i,0,0}$

$$b_{i,j,0} = \left(p_i^C\right)^j b_{i,0,0}, \quad \text{for } j \geq 0. \tag{15}$$

Additionally, every $b_{i,j,k}$ state can be represented as a function of $b_{i,j,0}$

$$b_{i,j,k} = \begin{cases} \dfrac{\mathrm{CW}_{i,j} + 1 - k}{\mathrm{CW}_{i,j} + 1} \dfrac{p_i^G p_i^B b_{i,-1,0} + b_{i,-2,0}}{1 - p_i^B}, & \text{for } j = 0, \ k \geq 1, \\[2mm] \dfrac{\mathrm{CW}_{i,j} + 1 - k}{\mathrm{CW}_{i,j} + 1} \dfrac{1}{1 - p_i^B} b_{i,j,0}, & \text{for } j \geq 1, \ k \geq 1. \end{cases} \tag{16}$$

Now, let us consider the case where there was a collision at the first backoff stage (c.f., Figure 2). We distinguish these Markov states by using the prime symbol. Analysing the chain, we see that

$$b_{i,1,0}' = p_i^G\left(1 - p_i^B\right) p_i^T b_{i,-1,0}. \tag{17}$$

Furthermore, every $b_{i,j,0}'$ state can be represented as a function of $b_{i,1,0}'$

$$b_{i,j,0}' = \left(p_i^C\right)^{j-1} b_{i,1,0}', \quad \text{for } j > 1. \tag{18}$$
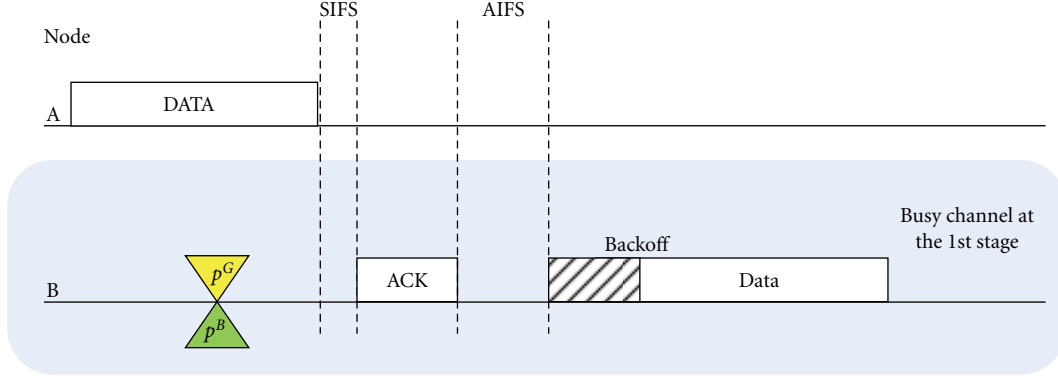
FIGURE 5: Diagram illustrating the action sequences related to a busy channel at the 1st stage.

Additionally, every $b'_{i,j,k}$ state can be represented as a function of $b'_{i,j,0}$

$$
b'_{i,j,k} = \begin{cases} \dfrac{CW_{i,j}+1-k}{CW_{i,j}+1}\dfrac{p_i^G\left(1-p_i^B\right)p_i^T b_{i,-1,0}}{1-p_i^B}, & \text{for } j=1,\ k\geq 1, \\[2ex] \dfrac{CW_{i,j}+1-k}{CW_{i,j}+1}\dfrac{1}{1-p_i^B}b'_{i,j,0}, & \text{for } j\geq 2,\ k\geq 1. \end{cases}
$$
(19)

Analysing the Markov chain, the nonsaturation state can be described using the following equation:

$$
b_{i,-1,0} = (1-\rho_i)
$$
$$
\times \frac{\left[\left(1-p_i^C\right)\left(\sum_{j=0}^{M-1}b_{i,j,0}+\sum_{j=1}^{M-1}b'_{i,j,0}\right)+b_{i,M,0}+b'_{i,M,0}\right]}{p_i^G\left[1-(1-\rho_i)\left(1-p_i^B\right)\left(1-p_i^T\right)\right]}.
$$
(20)

Finally, from the normalisation property, we have

$$
b_{i,-2,0} + b_{i,-1,0} + \sum_{j=0}^{M}b_{i,j,0} + \sum_{j=1}^{M}b'_{i,j,0}
$$
$$
+ \sum_{j=0}^{M}\sum_{k=1}^{CW_{i,j}}b_{i,j,k} + \sum_{j=1}^{M}\sum_{k=1}^{CW_{i,j}}b'_{i,j,k} = 1.
$$
(21)

The transmission probability in a slot time for the ith AC can be derived from the analysis of the Markov chain

$$
\tau_i = \sum_{j=0}^{M}b_{i,j,0} + \sum_{j=1}^{M}b'_{i,j,0} + b_{i,-1,0}p_i^G\left(1-p_i^B\right).
$$
(22)

Now, the remaining unknown variable from (14)–(22) is D_i which is a sum of the following components.

(i) The average countdown delay (D_i^{CD}), which is calculated as the sum of the time spent on counting down backoff slots after a collision or a busy channel at the first stage (this occurs with a probability of $[p_i^G(1-p_i^B)p_i^T(1-\rho_i)]$ or $[p_i^G p_i^B(1-\rho_i)+\rho_i]$, resp.).

The average time spent at each backoff stage j is $T_e(CW_{i,j}/2)$. Therefore, we have

$$
D_i^{CD} = p_i^G\left(1-p_i^B\right)p_i^T(1-\rho_i)
$$
$$
\times \sum_{j=1}^{M}\left(p_i^C\right)^{j-1}\left(1-p_i^C\right)\sum_{h=1}^{j}T_e\frac{CW_{i,h}}{2}
$$
$$
+ \left[p_i^G p_i^B(1-\rho_i)+\rho_i\right]
$$
$$
\times \sum_{j=0}^{M}\left(p_i^C\right)^{j}\left(1-p_i^C\right)\sum_{h=0}^{j}T_e\frac{CW_{i,h}}{2}.
$$
(23)

(ii) The average frame blocking delay (D_i^B)

$$
D_i^B = D_i^{CD}p_i^B\frac{P^S T^S + (p^B - P^S)T^C}{p^B T_e},
$$
(24)

where the quotient is the average time in which the node is blocked.

(iii) The average successful transmission delay (D_i^T), which is the product of the duration of a successful transmission (T^S) and the probability, that the frame is not dropped

$$
D_i^T = T^S\left\{1 - \left(p_i^C\right)\left[p_i^G\left(1-p_i^B\right)p_i^T\left(p_i^C\right)^{M}(1-\rho_i)\right.\right.
$$
$$
\left.\left. + \left(p_i^C\right)^{M+1}\left[p_i^G p_i^B(1-\rho_i)+\rho_i\right]\right]\right\}.
$$
(25)

(iv) The average retransmission delay (D_i^R), which can be calculated by taking into account the average number

of retransmission attempts j and the duration of a collision (T^C)

$$D_i^R = T^C\left(1 - p_i^C\right)$$

$$\times \left[\sum_{j=1}^{M} j\left(p_i^C\right)^{j-1} p_i^G\left(1 - p_i^B\right) p_i^T (1 - \rho_i) \right. \tag{26}$$

$$\left. + \sum_{j=0}^{M} j\left(p_i^C\right)^{j}\left[p_i^G p_i^B (1 - \rho_i) + \rho_i\right]\right].$$

(v) The average countdown delay of dropped frames from the ith AC which we define as

$$D_i^{\text{DROP}} = \left(p_i^C\right)^M\left(D_i'^{\text{CD}} + D_i'^{B} + D_i'^{R}\right). \tag{27}$$

The components of (27) are defined as follows. The average countdown delay of dropped frames ($D_i'^{\text{CD}}$)

$$D_i'^{\text{CD}} = T_e\left\{p_i^G\left(1 - p_i^B\right) p_i^T (1 - \rho_i) \sum_{j=1}^{M} \frac{\text{CW}_{i,j}}{2}\right.$$

$$\left. + \left[p_i^G p_i^B (1 - \rho_i) + \rho_i\right] \sum_{j=0}^{M} \frac{\text{CW}_{i,j}}{2}\right\}. \tag{28}$$

The average frame blocking delay of dropped frames ($D_i'^{B}$)

$$D_i'^{B} = D_i'^{\text{CD}} p_i^B \frac{P^S T^S + \left(p^B - P^S\right) T^C}{p^B T_e}. \tag{29}$$

The average retransmission delay of dropped frames ($D_i'^{R}$)

$$D_i'^{R} = T^C(M+1)\left[p_i^G\left(1 - p_i^B\right) p_i^T (1 - \rho_i)\right.$$

$$\left. + p_i^G p_i^B (1 - \rho_i) + \rho_i\right]. \tag{30}$$

Equations (28)–(30) resemble (23)–(25) but they take into account dropped frames (i.e., those which have been retransmitted M times).

We calculate the overall service time for the ith AC using the following equation:

$$D_i = D_i^{\text{CD}} + D_i^{B} + D_i^{R} + D_i^{T} + D_i^{\text{DROP}}. \tag{31}$$

This allows us to compute ρ_i (13). Then, we calculate τ_i as a function of p_i^B, p_i^G, p_i^C, p^T, and ρ_i using (2) and (14)–(22). Finally, we can calculate S_i using (1), (4), and (6)–(12).

4. Misbehaviour Analysis

For the analysis of misbehaviour, we focus on backoff misbehaviour, because our studies have shown that this type of misbehaviour gives significant throughput gains to selfish users in single-hop networks [6]. At the same time, it is easy to perform with modern wireless drivers [2]. We model

backoff misbehaviour by using an additional AC for which we set nonstandard CW_i^{MIN} and CW_i^{MAX} values. Therefore, in this paper, we consider an additional AC (indexed as m) with a nonstandard configuration. This approach allows us to consider networks with both well and misbehaving nodes.

We now use the proposed model to analyse the impact of backoff misbehaviour on node throughput. The analysis is done separately for saturation and nonsaturation conditions. In saturation, the following model parameters are known: $\rho_i = 1$, $p_i^G = 1$, and $p_i^T = 1$ for each AC used in the network. To simplify the calculations, we assume for all i : $\text{CW}_i^{\text{MIN}} = \text{CW}_i^{\text{MAX}} = \text{CW}_i$ and $p_i^C = p_i^B = p_i$, the misbehaving node is the only node in its AC ($n_m = 1$), and there is more than one node in the network. Without these simplifications, it would be significantly more difficult to perform the analysis. However, the simulation results presented in Section 5.3 lead to the same conclusions. Furthermore, assuming S_m is a continuous function of CW_m (similarly to [13]), we can calculate the following:

$$\frac{\partial S_m}{\partial \text{CW}_m} = \frac{\partial S_m}{\partial \tau_m} \frac{\partial \tau_m}{\partial \text{CW}_m}. \tag{32}$$

The first derivative of (6) can be computed as:

$$\frac{\partial S_m}{\partial \tau_m} = \frac{\left(c + 2T^C\right) T^{\text{DATA}}}{\left[(1 - \tau_m) T_e + c + \tau_m T^S + (1 - 2\tau_m) T^C\right]^2}, \tag{33}$$

where $c = \sum_{j=0 j \neq m}^{N_c - 1} n_j(1 - \tau_j)^{n_j - 1}(T^S + T^C)$. Similarly, we calculate

$$\frac{\partial \tau_m}{\partial \text{CW}_m} = \frac{2\left(p_m - 1\right)\left(1 + p_m + p_m^2 + p_m^3 + p_m^4\right)^2}{\left[3 - p_m \mathfrak{A} + \text{cw}_i + p_m(1 + p_m)\left(1 + p_m^2\right)\text{CW}_i\right]^2}, \tag{34}$$

where $\mathfrak{A}$ denotes $(3 + p_m + p_m^2 + p_m^3 + 2p_m^4)$. We conclude that $\partial S_m/\partial \tau_m > 0$, $\partial \tau_m/\partial \text{CW}_m < 0$, and thus throughput is a decreasing function of contention window size. Therefore, under saturation conditions a misbehaving node can increase its throughput by decreasing its backoff values.

Nonsaturation network conditions, however, are characterised by the fact that $S_m = \lambda_m$. This means that the achieved throughput is independent of CW_m. Therefore, under nonsaturation conditions a misbehaving node cannot increase its throughput by decreasing its contention window values.

5. Validation

The model was verified by comparing numerical and simulation results. We demonstrate that the model (1) behaves similarly to simulations, (2) outperforms three existing models, and (3) can be used for networks with misbehaving nodes. Therefore, the results presented in this paper confirm that the proposed model is valid.

The following analytical models were considered for comparison: Malone et al. [8], Engelstad and Osterbo [7], and Bianchi [16]. We refer to the models by the names of the first authors (*Malone*, *Engelstad*, and *Bianchi*). The first two

TABLE 2: Simulation parameters.

Basic rate	1 Mb/s	Data rate	11 Mb/s
δ	2 μs	Frame Size	1000 B
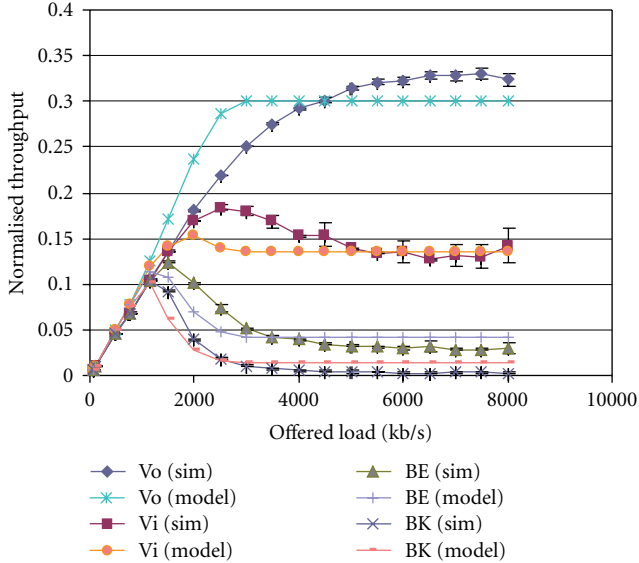
FIGURE 6: Throughput differentiation (one node per AC).

FIGURE 7: Throughput differentiation (multiple nodes per AC).

FIGURE 8: Variable frame size.

models were chosen because they support both saturation and nonsaturation conditions. Furthermore, all three were fairly simple and could be easily implemented. However, *Malone* and *Bianchi* are models of DCF and not EDCA. Therefore, the comparison with these models is performed only in scenarios in which a single AC is considered.

The simulations were performed with the ns-2 simulator and the EDCA patch from TKN Berlin [18]. This patch was modified to support misbehaving nodes. Additionally, significant discrepancies with the standard were corrected. Each simulation run was repeated many times to assure the defined confidence level. The 95% confidence interval of each simulation point is either presented in the figures or was too small for graphical representation.

In the following subsections, we considered several ad-hoc scenarios. In each scenario there was a single-hop network using the 802.11b physical layer. Tables 2 and 3 list the EDCA and simulation parameters, respectively.

5.1. Model Verification. First, we considered a simple scenario to verify the proposed model. The network consisted of four nodes, each transmitting one of the four ACs (Vo, Vi, BE, and BK). Figure 6 presents the normalised throughput with respect to the offered load. Both the simulation and analytical results are similar. The throughput increases linearly when the network is not saturated and is constant under saturation. This effect is correctly modelled for all ACs. Furthermore, the throughput differentiation of the four ACs is clearly visible in both theory and simulation.
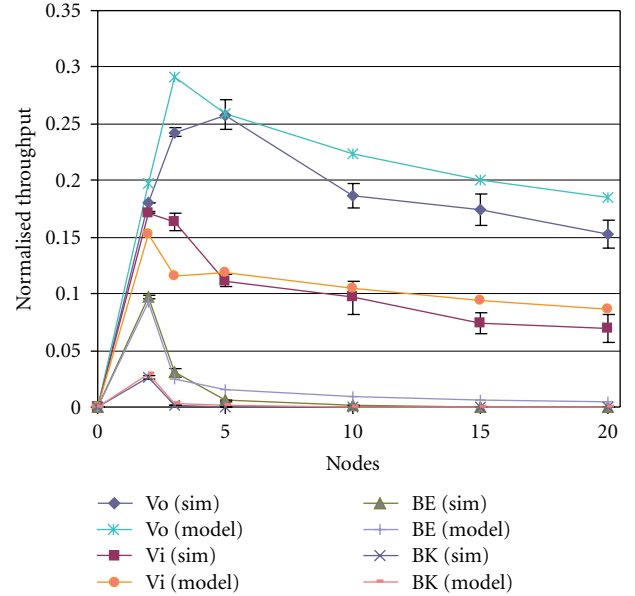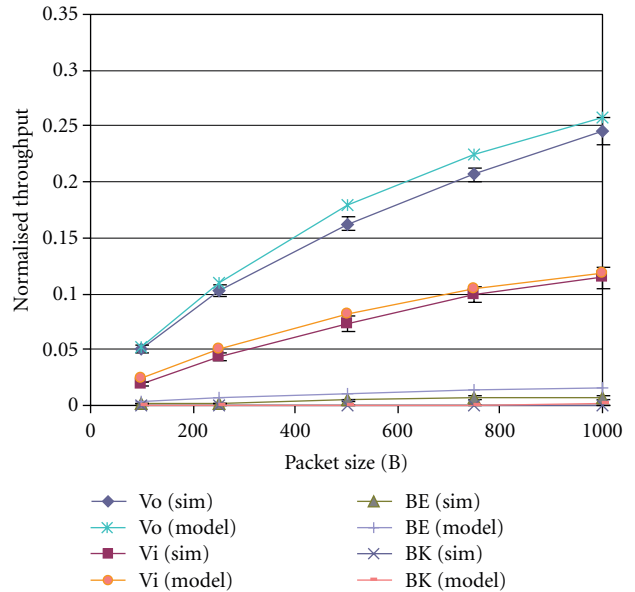
Next, we considered a scenario with an increasing number of nodes in the network. The number of nodes transmitting using each AC was constant. Each node generated 1000 kb/s of traffic. Therefore, we have a symmetrically increasing load. Figure 7 presents the normalised throughput with respect to the number of nodes per AC. Again, the analytical results correspond to the simulation results very well. This scenario confirms that our model is valid even when there is a high contention rate.

Finally, we tested the model in a scenario with varying frame sizes. There were 20 nodes in the network: five nodes
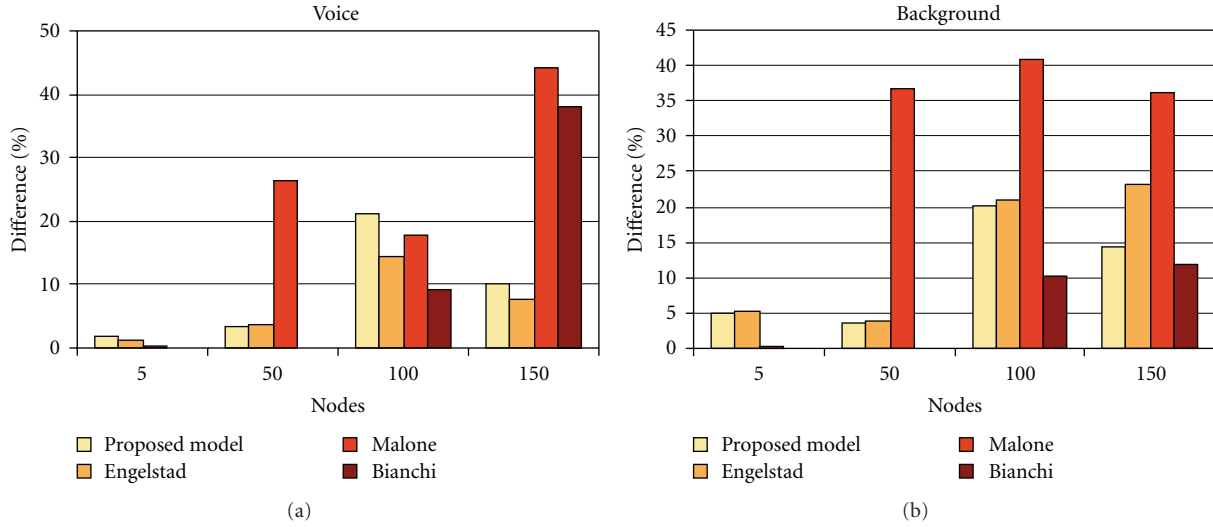
FIGURE 9: Comparison with other models (64 kb/s per-node offered load).
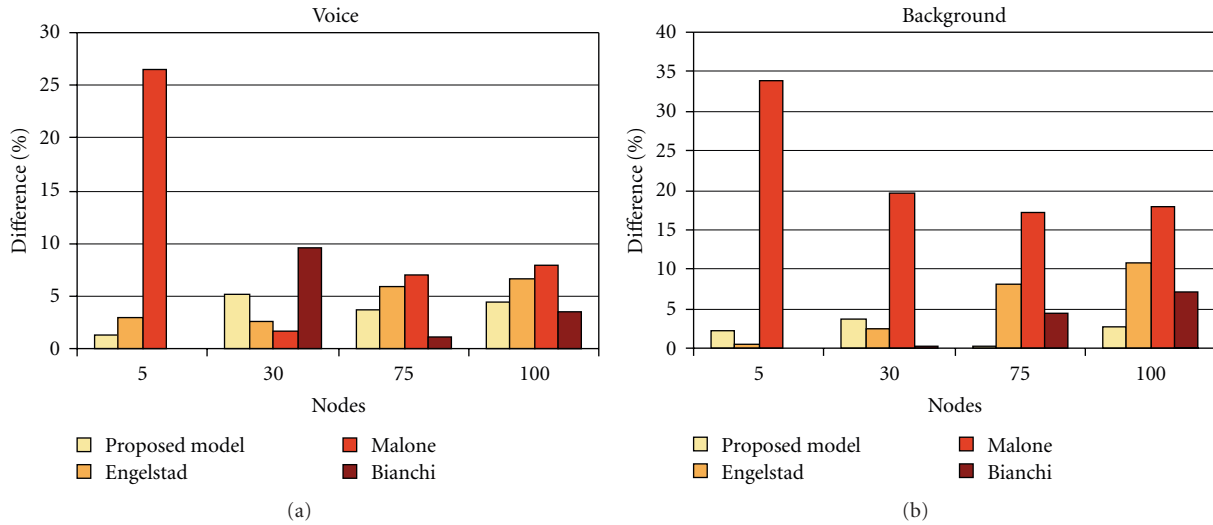

FIGURE 10: Comparison with other models (1000 kb/s per-node offered load).

transmitting data in each of the four ACs. Each node generated 1000 kb/s of traffic. Figure 8 presents the normalised throughput with respect to the frame size. The agreement between theory and simulations is very good for all tested frame sizes.

5.2. Comparison with Other Models. We compare our model with three other models (*Engelstad*, *Malone*, and *Bianchi*) in two scenarios. In the first scenario, we assume that each node in the network sends 64 kb/s of traffic in a given AC. Figure 9 presents the relative difference in throughput between the simulation results and the results obtained from the models for different network sizes. The relative difference is calculated as the absolute difference between the throughput values obtained analytically and by simulation divided by the simulation result. The results are given for two exemplary ACs: Voice and Background. Figure 10 presents

results from the second scenario, which differs in that nodes send 1000 kb/s of traffic. It is worth noting that since the *Bianchi* model was designed for saturation conditions, we present the results of this model only for networks with more than 100 (Figure 9) or 30 (Figure 10) nodes. To compare the results, we have summed the differences shown in Figures 9 and 10 in Table 3 for all but the *Bianchi* model (since it was tested only in saturation). Our model exhibits a good accuracy for both low and high offered loads. Furthermore, it is valid for both high- and low-priority ACs. Even for very large networks (up to 50 nodes), the difference does not exceed 5%. These results prove that it outperforms the other models.

5.3. Impact of Misbehaving Node. In the final set of simulations, we check if our model can cope with networks in which one of the nodes misbehaves by changing its contention

TABLE 3: Aggregate difference comparison.

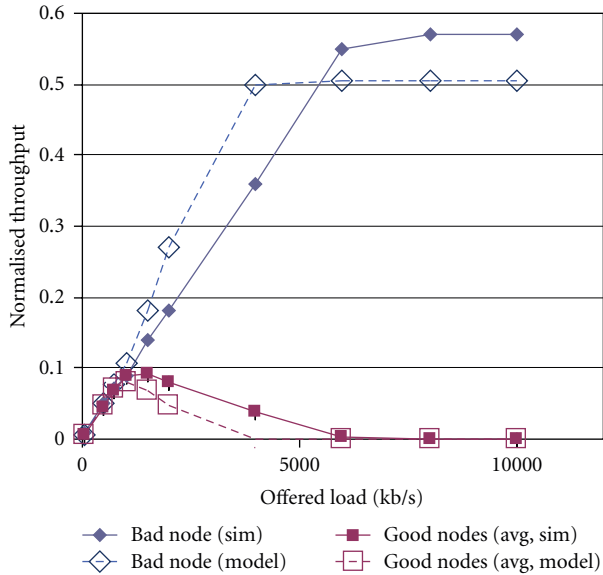| Per-node offered load	AC	Model			
		Proposed model	Engelstad	Malone	Bianchi
64 kb/s	Vo	36.57%	89.63%	89.09%	N/A
	BK	43.23%	53.50%	114.04%	N/A
1000 kb/s	Vo	14.52%	18.08%	42.99%	N/A
	BK	8.74%	21.99%	88.53%	N/A

FIGURE 11: Impact of contention window misbehaviour (good node throughput is averaged over the four good nodes).

window parameters. First, we test the model in a simple scenario. We assume that there are five nodes in the network. All of them are sending traffic of the BK AC. However, one of the nodes (the *bad* node) cheats by setting the following parameters: $CW^{MIN} = 1$ and $CW^{MAX} = 5$. Figure 11 presents the normalised throughput of the nodes with respect to the offered load. The main conclusion from the presented results is that the misbehaving node can easily dominate the network in terms of throughput. This occurs once the network reaches congestion (at a per-node offered load of approximately 1500 kb/s). Until that point the bad node's presence is not harmful. After reaching congestion, the bad node increases its throughput at the cost of the good nodes until saturation is achieved, in which the bad node obtains higher throughput than the average good node. Our model complies with the simulation results in a qualitative manner.

Next, we consider a more complex scenario in which we measure the impact of misbehaviour on higher priority traffic. Can a node misbehave by manipulating the parameters of a low-priority AC and deduct throughput from a high priority AC? To answer this question, a modified version of the previous scenario is analysed. There are also five nodes in the network; however, this time, four are sending traffic using the Vo AC (*good* nodes), and one node is using the

BK AC (*bad* node). Figure 12(a) presents the normalised throughput of the nodes with respect to the offered load in the case where there is no misbehaviour. The good nodes receive all the throughput, while the throughput of the bad node is significantly reduced. This is in line with the EDCA mechanism. If the bad node starts to misbehave (by setting $CW^{MIN} = 1$ and $CW^{MAX} = 5$) it obtains a significantly higher throughput then before, even higher than the good nodes (Figure 12(b)). The difference between this scenario, and the previous one is that the misbehaving node is not able to dominate the channel in the presence of Vo nodes (at least with contention window manipulation), as it was possible in the presence of other BK nodes. It can be inferred that despite the fact that Vo is the highest priority, it does not matter which AC the misbehaving node will manipulate— it is always able to benefit it terms of throughput. This kind of network behaviour can further influence the decision of a potentially malicious user to take advantage of the benefits of misbehaviour. Again, our model complies with the simulation results in a qualitative manner.

To determine the exact impact of the CW values the following scenario is analysed. We assume a network of five nodes in which each node generates traffic with an offered load of 8 Mbit/s. This assures saturation conditions. All nodes use the BK AC. However, the bad node manipulates its CW parameters. For ease of presentation, we assume that the bad node sets $CW^{MIN} = CW^{MAX}$ and varies it from 1 to 100. Figure 13 presents the normalised throughput of the nodes with respect to the configured contention window size. There is strong agreement between the analytical and simulation results. The misbehaving node achieves the highest throughput for the smallest CW parameters. Furthermore, its throughput decreases in an exponential manner with the increase of the contention window size. The point where the bad node's throughput is approximately equal to the average throughput of the good nodes occurs for $CW^{MIN} = CW^{MAX} = 50$. Since the 802.11 standard does not include any incentives for cooperation, a misbehaving user is free to chose the most profitable CW parameters (i.e., equal to 1).

In the final misbehaviour scenario, we analyse the impact of multiple noncolluding bad nodes on network performance. We consider a network of 20 nodes, each sending enough traffic to put the network into saturation. All nodes use the BK AC, however, the bad nodes set $CW^{MIN} = 1$ and $CW^{MAX} = 5$. Figure 14 presents the normalised average throughput of the nodes with respect to the percentage of misbehaving nodes in the network. Once more the analytical
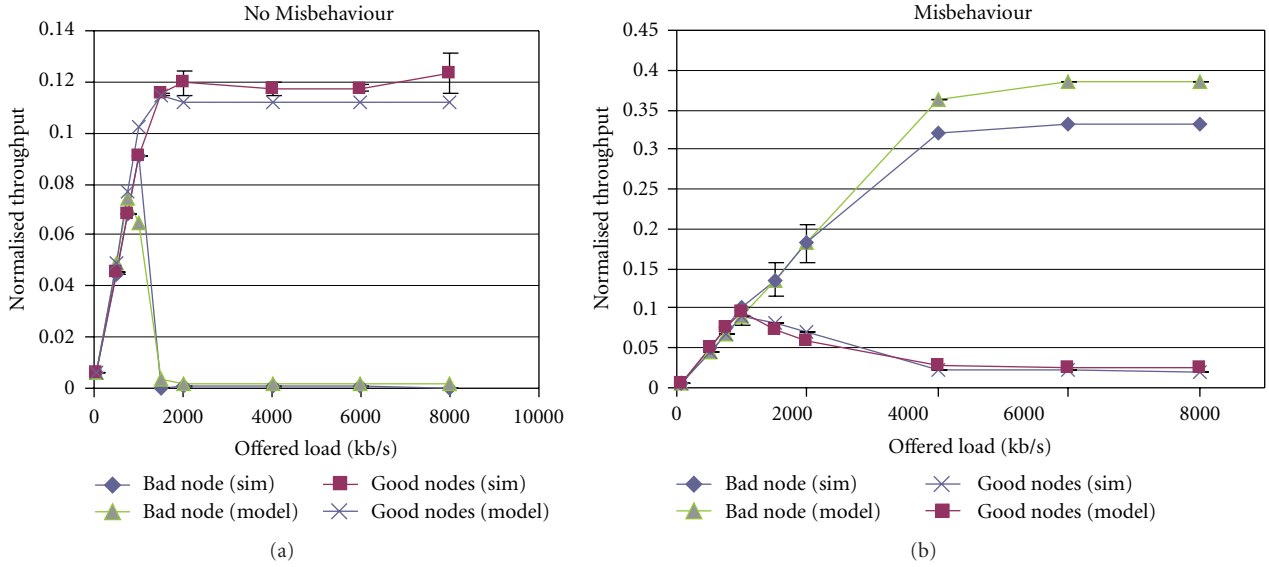
FIGURE 12: Impact of misbehaviour on higher priority traffic: (a) reference case, (b) misbehaviour case.
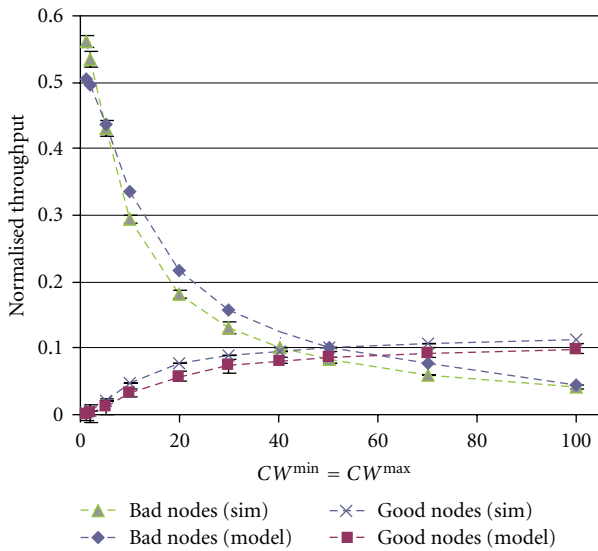

FIGURE 13: Impact of contention window size (good node throughput is averaged over the four good nodes).
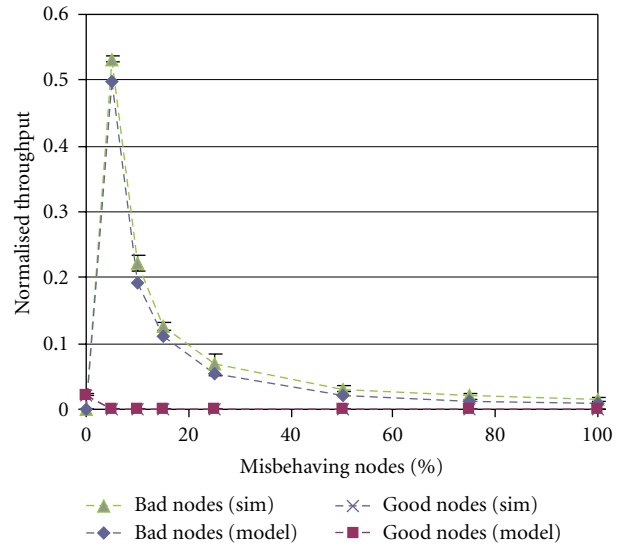

FIGURE 14: Impact of the percentage of misbehaving nodes in the network (throughput is averaged over the good and bad nodes).

results provided by the EDCA model closely resemble the simulation results. When there are no bad nodes in the network, each good node receives 0.02 of the normalised throughput. This small value is a result of the sharing of the medium by 20 homogeneous nodes. If there is at least one bad node in the network, the good nodes are almost deprived of any share in the network throughput. On the other hand, the throughput achieved by the bad nodes decreases exponentially with the increase of the percentage of misbehaving nodes in the network. This is because of the multiple collisions which result from the low CW values set by the bad nodes. Furthermore, these results show that if bad nodes comprise more than one-third of all nodes the network

performance (in terms of throughput) suffers considerably. Therefore, it is most advantageous to misbehave if there are none or very few misbehaving users in the network.

6. Conclusions

In this paper, we have presented a novel model of the IEEE 802.11 EDCA medium access function. Our model improves the existing solutions by supporting the following set of features: the ability to analyse networks with misbehaving nodes, support for saturation and nonsaturation network conditions, standard-compliant EDCA parameters, proper handling of frames, AIFS differentiation, and distinguishing

between the busy medium and frame blocking probabilities. Furthermore it is reasonably simple and, therefore, a possible candidate for further network analysis. We have verified the model by extensive simulation analysis and by comparing it to three other IEEE 802.11 models. Results show that our model behaves satisfactorily and outperforms other widely acknowledged models.

The main goal of the presented EDCA model is to be able to analyse networks with misbehaving nodes. In particular, we consider backoff misbehaviour. Again, a comparison with simulation results in several scenarios has proven that (a) our model performs correctly for scenarios with misbehaving nodes and (b) misbehaviour as a serious threat to WLANs. Our model is, therefore, a considerable contribution to the area of EDCA models and backoff misbehaviour. In particular, it can be used as the basis for enhancing EDCA to cope with misbehaviour. Furthermore, it can facilitate game theoretical analysis of IEEE 802.11 networks with misbehaving nodes (c.f., [10, 13]).

As future work, we envision extending the model to support multihop networks. Our previous results have shown that backoff misbehaviour in EDCA networks is a significant threat for multihop scenarios [5]. Therefore, a multihop analytical model of EDCA would be of assistance in studying such scenarios.

Nomenclature

AC:	Access Category,
AIFS:	Arbitration interframe space,
AIFSN_i:	Arbitration interframe space number for the ith AC,
$b_{i,j,k}$:	State distribution for $j \geq 0$,
$b_{i,-1,0}$:	Awaiting state for nonsaturation,
$b_{i,-2,0}$:	Awaiting state for saturation,
CW:	Contention window,
$\text{CW}_i^{\text{MIN}}, \text{CW}_i^{\text{MAX}}$:	CW minimum/maximum size for the ith AC,
$\text{CW}_{i,j}$:	CW size for the ith AC and jth retransmission attempt,
δ:	Propagation delay,
D_i:	Overall service time for the ith AC,
D_i^B:	Frame blocking delay for the ith AC,
D_i^{CD}:	Countdown delay for the ith AC,
D_i^{DROP}:	Frame dropping delay for the ith AC,
D_i^R:	Retransmission delay for the ith AC,
D_i^T:	Transmission delay for the ith AC,
H:	Length of the PHY and MAC overhead,
i:	AC number,
j:	Retransmission counter,
k:	Current CW value,
λ_i:	Traffic rate of the ith AC [frames per second],
n_i:	Number of nodes using the ith AC,
N_c:	Number of ACs,
p_i^C:	Frame collision probability for the ith AC,
p_i^B:	Frame blocking probability for the ith AC,
p_i^S:	Successful transmission probability for the ith AC,
p_i^G:	Frame generation probability for the ith AC,
p_i^T:	Probability of starting a frame transmission for the ith AC,
p^B:	Probability that a channel is busy,
P^S:	Probability of a successful transmission in any AC,
ρ_i:	Saturation probability for the ith AC,
S_i:	Throughput value for the ith AC,
τ_i:	Transmission probability in a slot time for the ith AC,
$T^{\text{ACK}}, T^{\text{CTS}}, T^{\text{RTS}}$:	Time required to send the ACK/CTS/RTS frame, respectively,
T^{DATA}:	Average time required to send a DATA frame,
T_e:	Slot time,
T^C, T^{CS}, T^S:	Duration of a collision/contention slot/successful transmission, respectively,
T^H:	Time required to send the PHY and MAC headers.

References

[1] "IEEE Standard for Information technology-Telecommunications and informationexchange between systems-Local and metropolitan area networks-Specific requirements—Part 11: Wireless LAN Medium Access Control(MAC) and Physical Layer (PHY) Specifications," IEEE Std 802.11-2007(Revision of IEEE Std 802.11-1999), 2007.

[2] Madwifi Project, http://madwifi-project.org/.

[3] G. Bianchi, A. Di Stefano, C. Giaconia, L. Scalia, G. Terrazzino, and I. Tinnirello, "Experimental assessment of the backoff behavior of commercialIEEE 802.11b network cards," in *Proceedings of the 26th IEEE International Conference on Computer Communications (INFOCOM '07)*, pp. 1181–1189, 2007.

[4] M. Raya, I. Aad, J. -P. Hubaux, and A. El Fawal, "DOMINO: detecting MAC layer greedy behavior in IEEE 802.11 hotspots," *IEEE Transactions on Mobile Computing*, vol. 5, no. 12, pp. 1691–1705, 2006.

[5] S. Szott, M. Natkaniec, and A. Banchs, "Impact of Misbehaviour on QoS in Wireless Mesh Networks," in *Proceedings of the International IFIP Networking Conference*, pp. 639–650, Springer, 2009.

[6] S. Szott, M. Natkaniec, R. Canonico, and A. R. Pach, "Impact of contention window cheating on single-hop IEEE 802.11e MANETs," in *Proceedings of the IEEE Wireless Communications and Networking Conference (WCNC '08)*, pp. 1356–1361, Las Vegas, Nev, USA, 2008.

[7] P. E. Engelstad and O. N. Osterbo, "Non-saturation and saturation analysisof IEEE 802.11e EDCA with starvation prediction," in *Proceedings of the 8th ACM International Symposium on Modeling, Analysis and Simulation of Wireless and Mobile Systems (MSWiM '05)*, pp. 224–233, 2005.

[8] D. Malone, K. Duffy, and D. Leith, "Modeling the 802.11 distributed coordination function in nonsaturated heterogeneous conditions," *IEEE/ACM Transactions on Networking*, vol. 15, no. 1, pp. 159–172, 2007.

[9] L. Guang, C. M. Assi, and A. Benslimane, "Enhancing IEEE 802.11 random backoff in selfish environments," *IEEE Transactions on Vehicular Technology*, vol. 57, no. 3, pp. 1806–1822, 2008.

[10] J. Konorski, "A game-theoretic study of CSMA/CA under a backoff attack," *IEEE/ACM Transactions on Networking*, vol. 14, no. 6, pp. 1167–1178, 2006.

[11] K. J. Park, J. Choi, K. Kang, and Y. C. Hu, "Malicious or selfish? Analysis of carrier sense misbehavior in IEEE 802.11 WLAN," *Quality of Service in Heterogeneous Networks*, vol. 22, pp. 351–362, 2009.

[12] R. D. Vallam, A. A. Franklin, and C. Siva Ram Murthy, "Modelling cooperative mac layer misbehaviour in ieee 802.11 ad hoc networks with heterogeneous loads," in *Proceedings of the 6th International Symposium on Modeling and Optimization in Mobile, Ad Hoc, and Wireless Networks and Workshops (WiOPT '08)*, pp. 197–206, 2008.

[13] M. Cagalj, S. Ganeriwal, I. Aad, and J. P. Hubaux, "On selfish behavior in CSMA/CA networks," in *Proceedings of the IEEE International Conference on Computer Communications (INFOCOM '05)*, pp. 2513–2524, March 2005.

[14] F. Peng, "Mobile networks: theoretical performance evaluation of EDCA in IEEE 802.11e wireless LANs," *European Transactions on Telecommunications*, vol. 21, no. 3, pp. 266–275, 2010.

[15] J. Hu, G. Min, M. Woodward, and W. Jia, "A comprehensive analytical model for IEEE 802.11e QoS differentiation schemes under unsaturated traffic loads," in *Proceedings of IEEE International Conference on Communications*, pp. 241–245, 2008.

[16] G. Bianchi, "Performance analysis of the IEEE 802.11 distributed coordination function," *IEEE Journal on Selected Areas in Communications*, vol. 18, no. 3, pp. 535–547, 2000.

[17] R. Motwani and P. Raghavan, *Randomized Algorithms*, Cambridge University Press, New York, NY, USA, 1995.

[18] S. Wiethoelter, M. Emmelmann, C. Hoene, and A. Wolisz, "TKN EDCA model for ns-2," Tech. Rep. TKN-06-003, Telecommunication Networks Group, Technische Universität Berlin, 2006.